

Prefectures vulnerable to water scarcity are not evenly distributed across China

Fubo Zhao¹, Xi Wang¹, Yiping Wu¹  [✉] & Shailesh Kumar Singh² 

Water scarcity has become a significant constraint to sustainable development. While the water scarcity has been widely assessed, its social impacts are infrequently evaluated. Here, we developed a framework to integrate the water scarcity and climate sensitivity to examine social vulnerability at the prefecture level across China. Results showed that 41% of the 301 prefectures were highly water stressed and 30% were highly sensitive to changing climate. We identified 44 hotspot prefectures using a combination of high water scarcity and climate sensitivity. We mapped the gradient in social vulnerability to water stress and climate sensitivity in these 44 prefectures and found that prefectures with 'very high' social vulnerability were primarily distributed in Central and Southwest China. These 'very high' vulnerable prefectures are home to more than 58 million people. The consideration of both water scarcity and climate sensitivity across management units has potential to formulate policies regarding water resources management.

¹Department of Earth & Environmental Science, School of Human Settlements and Civil Engineering, Xi'an Jiaotong University, 710049 Xi'an, Shaanxi Province, China. ²National Institute of Water and Atmospheric Research Ltd., Christchurch, New Zealand. ✉email: rocky.ypwu@gmail.com

The availability of freshwater resources is key to both environmental and socio-economic health of any region^{1,2}. With rapidly growing population and increasing urbanization, the gap between demand and supply of freshwater resources is steadily increasing, leading to significant water scarcity in many regions of the world^{3–7}. Severe water scarcity challenges food security^{8,9}, power generation¹⁰, and ecological restoration^{11,12}, and will potentially compromise the achievement of the United Nations Sustainable Development Goals (SDGs) (e.g., SDG6—clean water and sanitation, and SDG14—life below water). Therefore, understanding water scarcity is important for formulating effective policy at a range of spatial scales (global, regional, and local).

Since the late 1980s, when water scarcity was recognized as a worldwide problem, many indices have been developed to facilitate the assessment of water scarcity across the world⁸. The most used water scarcity index is the ratio of water demand to water supply, which is also called blue water scarcity, where blue water is usable freshwater that may be sourced from lakes, streams, and groundwater^{8,13}. Several studies have used this index to assess water resources and identify severe water scarcity in many regions of the world^{6,10,14–16}. However, this simple index only considers surface and groundwater availability, and ignores soil moisture (so-called green water)¹⁷. To overcome this shortcoming, some sophisticated indicators have been developed more recently, and these include the physical water scarcity index that integrated root zone water availability to reflect agricultural drought¹⁸ and the more complex water scarcity index, which recognized both freshwater availability, and quality constraints arising from pollution of water resources¹⁹. Although these indices are valuable for improving our understanding of water scarcity, they focus on one aspect of water scarcity and do not reflect the sensitivity of water conditions to climate change, now recognized as the most important factor influencing water resources^{20,21}. The uncertain effects of climate change on water scarcity have also raised concerns regarding the adequacy of current definitions of water scarcity^{22,23}. Moreover, freshwater scarcity assessments also typically consider one-side classification schemes which do not represent important variations in social sensitivities and responses²³. These approaches may have important limitations that constrain their ability to drive policy implementation regarding the actual and potential social impacts from the water-related crisis.

A widely used approach used to predict future water scarcity combines the output from hydrological models with climate projections from global climate models^{16,24–26}. The blue water resources predicted from hydrological models are then used to present water stress under future climate conditions. This approach has been frequently used at the global and regional scales under different water scenarios^{10,27}. This traditional forward approach is helpful to understand changes in water scarcity under climate change. However, the projections are not always helpful for formulating water policies because of various uncertainties, for example the large uncertainties in precipitation projections^{10,16,28}. To improve consideration of uncertainties in predictions of water resource availability, bottom-up approaches become important²⁹. Bottom-up approaches provide ways to explore changes in water availability and sensitivity to climate change without having to consider the specific (and uncertain) future projection of climate¹. Combining “bottom-up” scheme and exploratory modeling framework can thus provide direct information of how water availability will change, as well as ranges of likely vulnerability under various climate combinations.

In this study, we focus on assessments of water scarcity and sensitivity to climate change using a bottom-up framework. We combine survey-based water use data and remotely-sensed data to

address the following objectives: (1) Assess water scarcity conditions under the current climate and the sensitivity of water availability to climate change. (2) Analyze the co-occurrence of water scarcity and climate sensitivity and identify the hotspot regions suffering both high water stress and climate sensitivity. (3) Derive the gradient in social vulnerability to freshwater stress and climate sensitivity by inclusion of social adaptability. All analyses were performed at “small administrative unit scale”—in this case at prefecture level ($n = 301$) across China during 2000–2013.

Results

Water scarcity and sensitivity to changing climate. We mapped water scarcity conditions (average conditions of 2000–2013) and its sensitivity to climate change at the prefecture level (Fig. 1). Details of district distributions are shown in Supplementary Fig. 1. As shown in Fig. 1a, different levels of water scarcity occur in different regions. Prefectures that experienced water scarcity were mainly distributed in North China, with many prefectures in Huadong (HD), Huabei (HB), Huazhong (HZ), and Dongbei (DB) districts exhibiting high water scarcity ($WS > 0.4$). Statistically, 34, 23, 21, and 17 prefectures of HD, HZ, HB, and Dongbei (DB) districts suffered severe water shortage. HD district had the largest proportion (34 of total 76 prefectures, 45%) of high water scarcity. Regions where medium water scarcity occurred were largely in HD (20), Huanan (HN) (13), and HZ (12) districts (Fig. 1c). The Xinan (XN) district had the largest proportion of prefectures where low water stress occurred. At the national level, 41% (123), 24% (71), and 35% (107) prefectures were under high, medium, and low water scarcity, respectively, during the study period of 2000–2013.

Figure 1b shows the percentage of precipitation change (PC) (i.e., precipitation reduction) that resulted in a 25% reduction of WA with a fixed level of change in PE (15%). This framework can be used to easily test out various other scenarios. Changes in P and PE vs changes in WA were also shown in Supplementary Fig. 2. A lower PC indicated a higher sensitivity of WA to changing climate. In total, we found 30% of the selected 301 prefectures were highly sensitive to climate change according our classification. A decrease of no more than 5% in precipitation in these prefectures would cause water availability to decrease by a substantial 25%. These prefectures were more likely to suffer water stress under future climate, and they were mainly located in XN (26), DB (16), HB (15), HZ (11), and Xibei (XB) (11). Notably, in specific prefectures (Fig. 1b), a rise in P would cause a decline in WA despite the increase, as significant enhancements in PE within these dry and susceptible areas would counterbalance the increase in P^{30,31}, leading to a reduction in WA. 40% of prefectures (119) were found to be medially sensitive to climate change, with less than 10% (4.6–9.8%) decrease in precipitation led to a 25% decrease in water availability. These prefectures were widely distributed across China. The remaining 92 prefectures showed low sensitivities to climate change, with less than 22% (9.9–21.5%) decrease in precipitation led to a 25% decrease in water availability. These prefectures were primarily located in the lower reaches of the Yangtze River Basin, including large proportions of HD and HZ districts (Fig. 1d). Similar spatial patterns showing relatively higher climate sensitivity were also found for other tested threshold criteria (Supplementary Figs. 3 and 4).

Co-occurrence of water scarcity and climate sensitivity. We mapped the water scarcity conditions and climate sensitivities at the prefecture level and analyzed the co-occurrence of these phenomena (Fig. 2). We found that 30% (59) of 194 currently

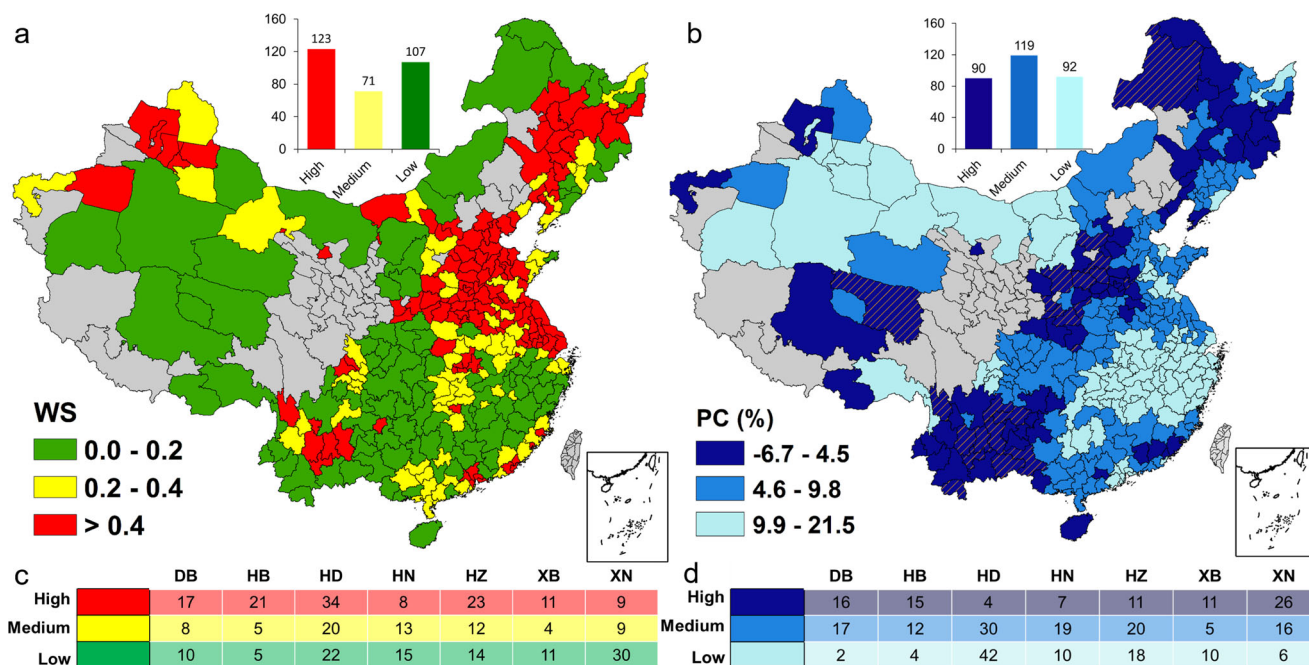


Fig. 1 Water scarcity and climate sensitivity of prefectures across China. **a** Water scarcity index (WS) derived from water demand to water availability (WA) of each prefecture. The WS classes were defined based on the WS values following ref. ¹⁰ low (<0.2), medium (0.2–0.4), and high (≥0.4). **b** Precipitation change (PC) (precipitation reduction) that caused a 25% reduction of WA. A lower PC indicates a higher sensitivity of WA to precipitation change (climate change). Values plotted on the color scales are categorized into three groups following ref. ³² high (≤PC₃₀, dark blue), medium (between PC₃₀ and PC₇₀, blue), and low (≥PC₇₀, shallow blue), in which PC_i represents the *i*th percentile of PC values. Shaded prefectures are ones with positive precipitation changes (negative precipitation reduction) that would still lead to WA reduction. **c** WS distribution and **d** PC distribution across districts of China. DB, HB, HD, HN, HZ, XB, and XN are abbreviations of different districts and the full description are shown in Supplementary Fig. 1. Gray-shaded prefectures are excluded from this study.

stressed prefectures (WS > 0.2) were simultaneously “highly sensitive” to climate change (i.e., highly sensitive to climate change in our classification). These prefectures were mainly located in HB, HD, DB, XN, HZ, and XB districts. Among these prefectures, 44 prefectures were also classified as highly water-stressed, which identified them as water-vulnerable hotspots—highly water-stressed prefectures with high sensitivity to climate change. A total of 170 million people were found within these prefectures (Supplementary Fig. 5). The hotspot prefectures were found across all districts of China, while the majority of these hotspot prefectures were located in HB (11), DB (10), HZ (9), and XN (6). 41% (80), and 29% (55) of 194 currently stressed prefectures exhibited “medium” and “low” sensitivity to climate change, respectively. The remaining 107 non-stressed prefectures were mainly located in the southern and northwestern portions of China. Among these prefectures, 33 were at the highest level (most) of climate sensitivity.

Social vulnerability to water scarcity and climate sensitivity. To better characterize social vulnerability, we placed the water scarcity and climate sensitivity in the context of social adaptability of each hotspot prefecture following ref. ²³ (Fig. 3). The aim of mapping the social vulnerability gradient is to minimize the social impacts of water stress and vulnerability to changing climate by identifying what prefectures with limited social adaptability are exposed to high water scarcity and climate sensitivity. The social vulnerability gradients were generated using threshold concept following ref. ³² and conducted across the 44 hotspot prefectures identified previously. Seven prefectures had high social adaptability and were identified as moderate vulnerable prefectures (yellow) (Fig. 3). These prefectures were mainly located in northern China, specifically the HB and DB districts. These

prefectures had a relatively higher adaptability to cope with actual water scarcity and potential water stress under changing climate and thus had a relatively lower risk suffering water crisis compared with others. In total, 22% of prefectures were at a high level of social vulnerability, and these were also concentrated in HB and DB districts. The prefectures with “very high” vulnerability level were concentrated in XN and HB districts (*n* = 15), which had a population of over 58 million people (Supplementary Fig. 5). These prefectures had lower capacities to adapt proactively and reactively to climate disturbance and would more easily suffer social harms (e.g., food shortages, social unrest, and others) due to water scarcity in a changing climate.

Discussion

Identifying regions that are suffering or likely to suffer water stress is important when making decisions regarding water resources planning and management. The spatial distribution of water scarcity conditions estimated in our study agreed with those in previous studies, with scarcity hotspots concentrated in northern China^{6,19,33–35}. The higher level of water scarcity is a consequence of both falling water supply and rising water demand because of increasing demand created by population growth and economic development in northern China³⁴. The decreasing surface water supply has led to the over-exploitation of groundwater resources, which has further exacerbated water scarcity, especially in the Huaihe River Basin of northern China³⁵. Previous studies were usually conducted at the grid or watershed scales to provide political guidance^{23,34}. However, many decisions regarding water management in China are still dependent on geophysical and economic conditions. For example, different measures could be made toward water management across the seven geophysical districts in China³⁶. In this study, we

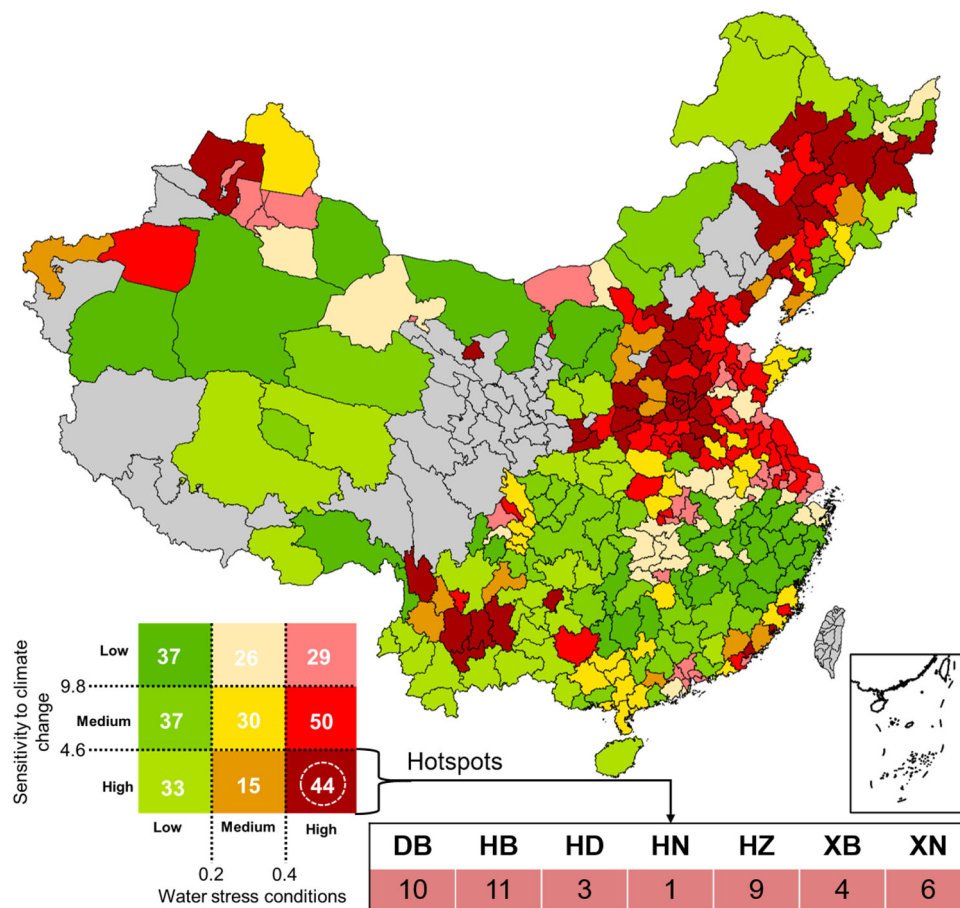


Fig. 2 Co-occurrence of water scarcity and climate sensitivity at the prefecture level. The dark red prefectures are identified as the vulnerable hotspot prefectures—high water-stressed and high sensitive to climate change according to our definition. Tables are the distributions of the 44 hotspots. DB, HB, HD, HN, HZ, XB, and XN are abbreviations of different districts and the full description are shown in Supplementary Fig. 1. Gray-shaded prefectures are excluded from this study.

conducted the analysis at the small administrative unit instead of topographically defined watersheds. Thus, the information derived from this study may be more suitable for guiding formulation of policy for water management, because these policies will better reflect or respond to the conditions likely to arise as a consequence of climate change, coupled with existing water scarcity.

Considering the uncertainties using traditional straightforward method to derive the sensitivity of water availability to climate change, we used a bottom-up approach in a Budyko framework. This approach can be effective in addressing the challenges posed by limited data and uncertainties associated with future precipitation change¹⁶. To further understand which are the main determinants of climate sensitivity of WA (represented as the PC magnitude in Fig. 1) in each prefecture, we conducted an importance analysis using a random forest machine learning algorithm from a total 24 physioclimatic (Supplementary Table 1) and socioeconomic characteristics for the selected 301 prefectures. As shown in Supplementary Fig. 6, the five most important factors were precipitation (factor importance of 39.2%), followed by elevation (DEM, 25.8%), air temperature (19.4%), potential evapotranspiration (PET, 17.1%), and economic development (denoted as GDP, 16.7%). Other variables related to vegetation, soil, and human activities were less important (less than 15.0%). In this sense, the background climate conditions are still primarily responsible for the WA sensitivity to changing climate for each prefecture of China, with elevation and

economic development playing secondary roles in determining climate sensitivity. These findings are consistent with those of previous studies. For example, the long-term climate and vegetation variables are key to water partitioning across India and Australia^{37,38}. Similarly, at the watershed scales, several studies also reported a more important role of climate change in driving runoff changes^{39,40}.

Our calculation procedure identified that 44 prefectures (representing 15% of the total) were hotspots—highly water-scarce prefectures were also most sensitive to changing climate. These 44 prefectures were representative because of their actual significant water scarcity and potential water stress under climate change. In other words, these originally water-stressed prefectures were also susceptible to changing climate. These hotspot prefectures can more easily suffer water shortage in a changing climate, which may exert potential negative impacts on the social system in these regions. For example, these regions may be linked with increased drought frequency when facing climate warming⁴¹, which are likely to exert large, undesirable influences on natural ecosystems and society. We further derived a social vulnerability gradient for each prefecture by including factors related to social adaptability. In general, vulnerability is core to generate risk^{42,43}. A higher vulnerability indicates that a system is more susceptible to potential hazards. Whereas vulnerability must be seen as situation-specific, interacting with a hazard event to generate risk⁴⁴. Vulnerability to actual and potential water stresses in our study, for example, does not infer vulnerability to

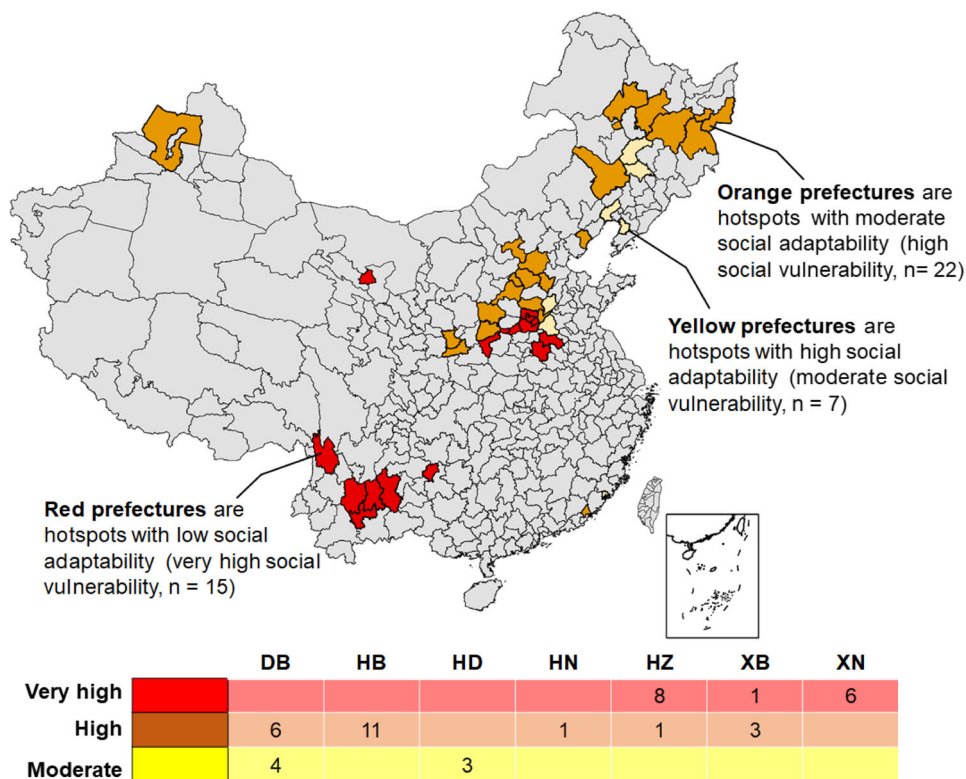


Fig. 3 Gradient of social vulnerability derived from the combination of water scarcity, climate sensitivity, and social adaptability. The “very high” vulnerability was derived by combining high water scarcity, high sensitivity, and low social adaptability; the “high” vulnerability was derived by combining high water scarcity, high vulnerability, and moderate social adaptability; the “moderate” vulnerability was derived by combining high water scarcity, high vulnerability, and high social adaptability. The vulnerable gradients were only conducted in the 44 hotspot prefectures. Hotspot prefectures (hotspots) are the ones with both high water scarcity and high climate sensitivity. Table shows the distribution of different vulnerability gradients among the seven districts in China.

other crisis (e.g., financial, hurricanes, earthquake, foods, and others). The identification of social vulnerability is of great importance for risk prevention and response related to freshwater variations. Lower social adaptability is usually linked with lower technological and economic capacity to cope with increasing water stress arising from climate change. Prefectures with very high vulnerability ($n = 15$) were mainly found in Southwest and North China, which are also the hotspot areas of drought^{30,45–47}. These prefectures should be used as pilot regions when implementing political actions (e.g., commissioning water resources projects) arising from water resources planning and management in response to climate change. The majority of moderately and highly vulnerable prefectures were found in North and Northeast China. However, these prefectures have relatively higher capacity to respond and adapt to freshwater stress under climate change.

It is worth mentioning that this study has some limitations. First, we only considered water stress across prefectures of China from the perspective of water quantity. In reality, water pollution is also exacerbating China’s water scarcity¹⁹. Pending data availability, water quality should also be considered in future water assessments. Second, we calculated water scarcity index values using freshwater stress and vulnerability to climate change due to data availability, ignoring indirect and non-local impacts such as the virtual water trade, which is increasingly likely to have an important impact on water and food security⁴⁸. This study only focused on natural water supply (P) and demand (AE) at the prefecture level to analyze climate sensitivity and vulnerability. It did not take into account human activities, such as garden and park construction, cropland irrigation, city green space construction, and artificial storage in reservoirs and dams. Taking into account these

additional elements to estimate WA and climate sensitivity would require a holistic approach, which was beyond the scope of this study. Third, this analysis was conducted at the mean annual level and therefore did not reflect inter-annual and seasonal variability in water stress and vulnerability. Future studies should consider the annual or seasonal water status and its sensitivity to climate change using such a framework. Finally, our calculation procedure (i.e., the simple threshold classification approach) may have deficiencies in identifying the hotspot prefectures. For example, numbers of prefectures suffering high water scarcity and climate sensitivity might be more or less if we use other classification methods^{23,32}. Future studies could consider more classification methods to gain a comprehensive insight of vulnerable regimes. Furthermore, due to the physical constraints of the Budyko method, we excluded 40 prefectures located primarily in the XB, HD, and HN districts from our analysis. This exclusion may introduce some uncertainties in identifying hotspot prefectures that are vulnerable to climate change. Nonetheless, because we found multiple lines of climate sensitivities of WA using different thresholds, we do not expect these uncertainties to affect our key identifications of hotspot-vulnerable prefectures among the selected 301 prefectures. Pending fine-scale statistical data availability, one can conduct more comprehensive and holistic analysis using our integrated framework. Despite these limitations, this study provides a first order estimation of the spatial variability of social vulnerability to actual and potential water stress of regions under changing climate.

Conclusions. In this study, we performed an explicit water scarcity assessment by considering water stress condition and

climate sensitivity at the small administrative unit—prefecture level in China. The climate sensitivity of WA was quantified using a Budyko-based bottom-up approach. Results showed that 41% prefectures (123 of the selected total 301 prefectures) were highly water-stressed and these were primarily distributed in North, Northeast, and Southwest China under current climate condition (2000–2013). Twenty-four percent (71) of prefectures were at the moderate levels of water scarcity. Sensitivity analysis showed that 30% (90) of prefectures were likely to be highly sensitive to changing climate. In total, 40% (119) and 30% (92) of prefectures were at the moderate and least levels of climate sensitivity, respectively. By analyzing the co-occurrence of water scarcity conditions and climate sensitivities, we identified 44 water-vulnerable hotspot prefectures—ones that are currently highly water-stressed and most sensitive to climate change. We further derived social vulnerability gradients by combining social adaptability among these 44 hotspot prefectures and found the prefectures with “very high” social vulnerability were primarily located in Southwest and Central China, while the prefectures with “high” and “moderate” social vulnerabilities were located in North and Northeast China. The ability to identify vulnerable hotspot prefectures and rank these along a vulnerability gradient has implications when formulating water policies regarding water resource management under climate change. The framework developed in this study can be applied in any regions where data are available to provide a first order estimation of the social vulnerability to actual and potential water stresses of a region, which information may be used in turn to develop appropriate policy.

Methods

We follow a three-step procedure to conduct the water scarcity, climate sensitivity, and social vulnerability analysis across all prefectures of China (Supplementary Fig. 7). In step 1, we used the historical records of meteorological information to verify the Fu’s Budyko function and estimate the water availability (represented by long-term P minus AE) across all prefectures of China. We then applied the statistic water abstraction data of each prefecture collected from ref. 49 to evaluate the water scarcity conditions. In step 2, a Budyko-based bottom-up approach was applied to estimate the critical climate thresholds for a selected change in water availability across China. In this step, the sensitivity of water availability to changing climate was identified according to changes in water availability and climate. The hotspot prefectures were also identified through analyzing the co-occurrence of water scarcity and climate sensitivity. In step 3, we conducted the social vulnerability analysis by integrating social adaptability across the hotspot prefectures identified in step 2. In this study, vulnerability represents the likelihood of society to experience harms due to exposure to actual and potential freshwater stresses under climate change. Identifying the gradient of social vulnerability to water stress and climate sensitivity is critical for adapting proactively and reactively to actual and potential water stresses to alleviate the water-related crisis under climate change. This initiative would help protect the weak part of the society, especially the one in developing countries such as China, when facing water-related hazards. We begin our methodological description with the Budyko framework. Following this, we describe the water scarcity assessment and climate sensitivity analysis. Finally, we derive the social vulnerability gradient for related prefectures to provide guidance for water resources management under climate change. For easily understanding of the terminologies used in our study, we provided a list of related definitions in Supplementary Table 2.

A Budyko-based framework for water availability estimation. We estimate long-term water availability (WA), defined as long-term precipitation (P) minus actual evapotranspiration (AE)⁵⁰ (ignoring long-term changes in water storage), across all prefectures using the Budyko water balance framework^{51,52}. The Budyko curve was developed on the basis of the water balance principle at the watershed scale. Specifically, the function depicts the relationship between long-term water availability (AE/P) and long-term climatic condition (long-term potential evapotranspiration (PE) to long-term P). Note that the original non-parametric Budyko relationship has been found to be applicable only over large temporal and spatial scales (>1 year; >10,000 km²), whereas the parametric function can be potentially applied to a wide range of spatial and temporal scales, provided that the curve’s parameters are appropriately calibrated and validated⁵³. Actually, the hydrology-climate relationship of a region can be regarded as a steady state when the study period is longer than 5–10 years and the Budyko water balance framework can be applied for water availability estimation⁵⁴. Despite the simple and “lumped

parameter” structure, the Budyko functions have proven effective in explaining and predicting changes in the terrestrial hydrological cycle across various spatial and temporal scales^{16,37,55–59} (Supplementary Table 3). Here, we employ a form of the Budyko curve of Fu⁵¹ with one parameter (ω) estimate the water availability using the input long-term P minus E through the water balance principle, assuming long-term variations of water storage do not change significantly between years (or different study periods):

$$\frac{AE}{P} = 1 + \frac{PE}{P} - \left(1 + \left(\frac{PE}{P}\right)^\omega\right)^{1/\omega} \quad (1)$$

The long-term climatic condition is represented by PE/P and the water availability is represented by AE/P. Water availability (WA) is thus defined as P-AE. Parameter ω , which modifies the steady-state hydrology-climate relationship at the mean annual scale, integrates the effects of biogeophysical features on water availability, such as the terrain, vegetation, and soil information³⁷. We derived the parameter ω using relevant datasets for the period 2000–2013, which was validated for applicability in estimating water availability using datasets from 1982–1999. To validate the estimation of WA during 2000–2013, we further collected runoff data from CNRD⁶⁰ and GRUN⁶¹ and compared them against the predictions. Also, we conducted cross-validations at the different spatial scales over China. The full validation process is shown in Supplementary Note 1 and Supplementary Figs. 8–11.

Water scarcity assessment. Following previous studies^{6,10,23}, we defined the water scarcity as the ratio of water abstraction to WA:

$$WS = \frac{WD}{WA} \quad (2)$$

where WS is water scarcity index and WD is total water abstraction. Data of water abstraction for each prefecture were collected from ref. 49. The water abstraction includes irrigation, industrial, urban, and rural water uses, which together account for more than 93% of total blue water abstraction⁴⁹. WA is estimated by the probabilistic Budyko function. Water scarcity is classed into three levels based on values of WS following previous studies^{2,4,10}: low water scarcity (<0.2) (or no water scarcity), medium water scarcity (0.2–0.4), and high water scarcity (≥ 0.4).

Climate-sensitivity analysis. We used a bottom-up approach based on a previous study¹⁶ to undertake a climate sensitivity analysis. The bottom-up approach was developed to confront the challenges arising from the unpredictable variations in precipitation patterns that may occur in the future. Applying the bottom-up approach offers an approach to investigate alterations in water availability regardless of future climate projections. This study utilizes exploratory modeling analysis with the bottom-up approach to evaluate a diverse spectrum of potential future climates and recognize combinations that may result in vulnerable water availability regimes⁶². The bottom-up approach begins with identification of ranges of water availability that represent vulnerability, followed by identification of climate conditions that are likely to cause this vulnerability^{16,29}, which differs from the traditional simple approach. First, we identified potential future climate scenarios by analyzing variations in precipitation and temperature (represented by PE) across all prefectures in China. The different climate combinations were generated according to the latest Intergovernmental Panel on Climate Change report in East Asia and Tibetan Plateau regions⁶³. The 5%–95% range of precipitation and air temperature changes in East Asian and Tibetan Plateau region was between –20 to 40% and 0 to 9 °C⁶⁴, respectively. We thus varied the P and PE (a proxy of temperature) from –40 to 75% and 0 to 30% to provide a wider climate space that covered the one predicted by global climate models. We obtained 10,000 potential climate combinations for each prefecture by sampling 100 equidistant values of P and PE, offering a comprehensive representation of possible future climate changes. Finally, the 10,000 possible climate combinations were used to estimate WA based on Budyko function. Then, we used above-mentioned Budyko function to project the WA change under various climate combinations. Finally, we identified the critical climate thresholds that led to a decrease of water availability below a selected level (i.e., 25% reductions in WA in this study and other scenarios can be tested with this framework). Note that we fixed PE at a 15% increase while vary P from –40 to 75% when estimating WA. We fixed PE by assuming that climate warming would certainly occur while the changes in precipitation would be uncertain according to the IPCC report⁶⁴. In this way, we derived the gradient of WA sensitivity to changing precipitation of all prefectures by comparing magnitudes of P reductions across all prefectures. For example, the smaller the decrease in P, the more sensitive the WA to changing climate (higher sensitivity). This approach thus helped identify the regions which were more likely to suffer water stress under future climate. Following a previous study⁶⁵, we used the 30th and 70th percentiles of relative reductions of P (%) to derive three sensitivity levels: least, moderate, and most. The simple use of the 30th and 70th percentiles is based upon the wet and dry identification according to precipitation changing regimes adopted by Allan et al.⁶⁶ and subsequently applied by Liu and Allan⁶⁷. A similar threshold-based classification of precipitation change has used elsewhere with success^{68,69}. We then investigated the co-occurrence of WS and climate sensitivity across all prefectures to identify the hotspot prefectures that were suffering high water stress and climate sensitivity.

Dominant factors for climate sensitivity. Understanding the mechanism of the sensitivity of WA to changing climate is critical for formulating appropriate measures for water resources management across different prefectures. For example, measures such as seawater desalination or virtual water trade could be applied for coastal prefectures (e.g., prefectures in HD, DB, and HN districts in our study), while other measures such as water transfer project, groundwater exploitation, or reservoir construction could be made for inland prefectures (e.g., prefectures in HB, HZ, XN, and XB districts in our study) to alleviate water crisis in terms of the different driving forces of water availability⁷⁰. Therefore, to better understand the dominant factors of sensitivity of WA to changing climate, we applied a random forest machine learning algorithm to conduct the importance analysis from a total 24 physioclimatic and socioeconomic factors for each prefecture (Supplementary Table 1). Random forest is a popular machine learning model based on an ensemble of regression trees for classification or regression and produce an assessment of variable importance^{71,72}. This approach has been widely used in hydrological prediction and variable importance identification^{73–76}. The independent variables used in our study were selected based on previous studies^{37,54,77–84} and they are closely related to variations in water availability³⁷. Among the 24 variables, seven are related to climate, five are related to topography, five are related to vegetation, three are related to soil, three are related to human activities, and one is related to economic development (see Supplementary Table 1).

Derivation of social vulnerability gradients. While there is considerable consensus around the general principles of vulnerability⁸⁵, we based on the vulnerability definition proposed by Turner et al.⁸⁶ and Cardona and Carreño⁸⁷. The concept of vulnerability generated by Cardona and Carreño⁸⁷ has been adopted also in the 2009 UNISDR terminology⁸⁸. Our study follows a similar approach to that of refs. ⁸⁹ and ²³, who conducted a global assessment of river basin resilience using social-ecological principles. However, we focus specifically on the potential social impacts of freshwater stress and climate sensitivities, rather than conducting a broad evaluation of prefecture resistance to a wide range of vulnerabilities. Our study thus has a narrower, more specific scope. In our study, we conceptualized social vulnerability as the combination of (i) exposure to freshwater stress, (ii) climate sensitivity (potential water stress), and (iii) social adaptive capability. Specifically, we first derived water scarcity and sensitivity of available water resources to changing climate and then identified the hotspot prefectures according to the co-occurrence of water scarcity and vulnerability. The hotspots were identified as the prefectures that were suffering both high water scarcity and climate sensitivity (section “water scarcity assessment” and “climate-sensitivity analysis”). On this basis, we subsequently incorporated social adaptability datasets (from ref. ⁸⁹), to derive social vulnerability gradients across the hotspot prefectures in China. The social adaptability, or adaptive capacity, represents “the ability of the system to respond to disturbances”. Varis et al.⁸⁹ derived adaptive capacity using the indicators of governance (government effectiveness), economic strength (Gross Domestic Production per capita purchasing power parity)⁹⁰, and human development (human development index)⁹⁰ by equal weight composite method. We note that this is a relatively parsimonious conceptualization of adaptive capacity which may be challenged to represent critical dynamic properties of the social system, such as its transformability. The dataset has been used to examine the social and ecological impacts of freshwater stress across various global basins²³. By considering social adaptability, it is possible to obtain more accurate estimates of vulnerable social activities that may be affected by the co-occurrence of freshwater stress and climate sensitivity. A lower value of social adaptability index indicates lower ability of a vulnerable prefecture to adapt to disturbance arising from future climate change. We also consistently used the 30th and 70th percentiles as thresholds to derive three adaptability levels: low, moderate, and high. As we based our analysis on three regimes (i.e., water scarcity, climate sensitivity, and social adaptability), this threshold scheme provided a necessary and rather simple configuration for the relative assessment of social vulnerability for this study³². Following this, we derived three levels of social vulnerability across the hotspot prefectures: very high, high, and moderate. The “very high” vulnerability was derived by combining high water scarcity, high sensitivity, and low social adaptability; the “high” vulnerability was derived by combining high water scarcity, high vulnerability, and moderate social adaptability; the “moderate” vulnerability was derived by combining high water scarcity, high vulnerability, and high social adaptability. In terms of the classifications, a higher level of social vulnerability indicate a social system of a prefecture is more susceptible to actual and potential water stresses under climate change. It should be noted that the social vulnerability was only applied in the identified hotspot prefectures instead of all related prefectures. We here focused on the social vulnerability to water-related risk analysis and the water issues (i.e., actual and potential water stresses) should be solved before defining social vulnerability. In our study, the identified hotspot prefectures according to water scarcity and climate sensitivity conditions can be regarded as the ones with water problems. The vulnerability analysis was thus applied in these prefectures regarding urgent and efficient measures for water resources management in these regions. Social vulnerability, in our terminology, thus represents the capacity of a society to cope with critical water issues to minimize the social impacts of actual and potential water stresses under climate change.

Study area and data. The methodology was tested at the small political unit level—prefectures—in mainland China. In total, there are 341 prefectures in mainland China, whose areas range from 457 km² to 471,450 km². We first selected

Table 1 Long-term meteorological information and statistics of ω parameter.

| Variables | Mean | Maximum | Median | Minimum |
|-----------|------|---------|--------|---------|
| P (mm) | 1028 | 2229 | 984 | 93 |
| AE (mm) | 625 | 1263 | 635 | 42 |
| PE (mm) | 1009 | 1376 | 1009 | 622 |
| AI | 1.5 | 12.1 | 1.0 | 0.5 |
| ω | 2.6 | 6.1 | 2.3 | 1.1 |

prefectures according to the Budyko space following Singh and Kumar¹⁶. We removed the prefectures where the physical constraints of atmospheric water supply and demand laws did not apply (Supplementary Fig. 12). Based on this principle, 301 prefectures were finally selected for analysis. The remaining prefectures were then grouped into seven districts (higher-level political units) according to geophysical and economic conditions of China. Finally, seven districts were identified—HN, XN, HZ, DB, HZ, HB, and XB, which together cover the entire land mass of China. Data of water abstraction, including irrigation, industrial, urban, and rural water uses, were collected from ref. ⁴⁹. The data were compiled at the prefecture level and covered our study period of 2000–2013.

Data required to construct the Budyko framework include long-term P, PE, and AE. The long-term P was obtained from the China Meteorological Forcing Dataset, which was produced by the Institute of Tibetan Plateau Research, Chinese Academy of Sciences⁹¹. The dataset was generated by combining remote sensing products, reanalysis datasets, and in-situ observation data from weather stations. It covers the period from 1982 to 2013, and has a spatial resolution of 0.1°. The long-term PE was estimated using the Penman–Monteith equation^{92,93} (Eq. (3)) based on the meteorological information from weather stations across China. This equation is a standard version for PE calculation of the Food and Agriculture Organization (FAO)⁹⁴ and is adapted to be representative for a hypothetical crop surface with assumed height of 0.12 m, surface resistance of 70 s m⁻¹, and an albedo of 0.23 as follows:

$$PE = \frac{0.408\Delta(R_n - G) + \frac{900}{T+273}\gamma u_2 (e_s - e_a)}{\Delta + \gamma(1 + 0.34u_2)} \quad (3)$$

where R_n is net radiation at the crop surface (MJ m⁻² day⁻¹), G is the soil heat flux density (MJ m⁻² day⁻¹), T is the daily air temperature at 2 m height (°C), u_2 is the wind speed at 2 m height (m s⁻¹), e_s and e_a is the saturation and actual vapor pressure (kPa), γ is psychrometric constant (kPa °C⁻¹), and Δ is slope vapor pressure curve (kPa °C⁻¹). A Kriging method was used to interpolate station-based PE to a 0.1° resolution. The long-term AE (1982–2013) was collected from ref. ⁹⁵, with a spatial resolution of 0.073°. The AE products from ref. ⁹⁵ have been widely used in water availability analysis^{37,96–98}. The social adaptability data were obtained from ref. ⁸⁹. All data were resampled to 0.1° spatial resolution before analysis. We use the latest period of 2000–2013 as the reference period to conduct the analysis. The long-term meteorological information and generated ω parameter are listed in Table 1.

Data availability

The precipitation data were obtained from the National Tibetan Plateau Data Center (<http://data.tnpc.ac.cn>). Other meteorological data that were used for potential evapotranspiration estimation were collected from the China Meteorological Data Service Center (<http://data.cma.cn>). Other datasets are available at Figshare (https://figshare.com/articles/dataset/CityClass_RandomForest_FigShare/22323751).

Code availability

The codes used for the analyses are available from the corresponding author. All code is developed in R.

Received: 25 August 2022; Accepted: 17 April 2023;

Published online: 28 April 2023

References

1. Singh, R., Wagener, T., Crane, R., Mann, M. E. & Ning, L. A vulnerability driven approach to identify adverse climate and land use change combinations for critical hydrologic indicator thresholds: application to a watershed in Pennsylvania, USA. *Water Resour. Res.* **50**, 3409–3427 (2014).

2. Liu, J. et al. Water scarcity assessments in the past, present, and future. *Earth's Future* **5**, 545–559 (2017).
3. Munia, H. et al. Water stress in global transboundary river basins: significance of upstream water use on downstream stress. *Environ. Res. Lett.* **11**, <https://doi.org/10.1088/1748-9326/11/1/014002> (2016).
4. Wada, Y. et al. Global monthly water stress: 2. Water demand and severity of water stress. *Water Resour. Res.* **47**, <https://doi.org/10.1029/2010wr009792> (2011).
5. Yin, Y. et al. Quantifying water scarcity in northern China within the context of climatic and societal changes and south-to-north water diversion. *Earth's Future* <https://doi.org/10.1029/2020ef001492> (2020).
6. Liu, X. et al. A spatially explicit assessment of growing water stress in China from the past to the future. *Earth's Future* **7**, 1027–1043 (2019).
7. Qin, Y. et al. Flexibility and intensity of global water use. *Nat. Sustain.* **2**, 515–523 (2019).
8. Liu, W., Liu, X., Yang, H., Ciais, P. & Wada, Y. Global water scarcity assessment incorporating green water in crop production. *Water Resour. Res.* **58**, <https://doi.org/10.1029/2020wr028570> (2022).
9. Rockström, J. et al. Future water availability for global food production: The potential of green water for increasing resilience to global change. *Water Resour. Res.* **45**, <https://doi.org/10.1029/2007WR006767> (2009).
10. Greve, P. et al. Global assessment of water challenges under uncertainty in water scarcity projections. *Nat. Sustain.* **1**, 486–494 (2018).
11. Feng, X. et al. Revegetation in China's Loess Plateau is approaching sustainable water resource limits. *Nat. Clim. Change* **6**, 1019–1022 (2016).
12. Zhao, F., Wu, Y., Yin, X., Alexandrov, G. & Qiu, L. Toward sustainable revegetation in the loess plateau using coupled water and carbon management. *Engineering* **15**, 143–153 (2022).
13. Cai, J., Varis, O. & Yin, H. China's water resources vulnerability: a spatio-temporal analysis during 2003–2013. *J. Clean. Prod.* **142**, 2901–2910 (2017).
14. Hanasaki, N. et al. A global water scarcity assessment under Shared Socio-economic Pathways—Part 2: water availability and scarcity. *Hydrol. Earth Syst. Sci.* **17**, 2393–2413 (2013).
15. Hanasaki, N., Yoshikawa, S., Pokhrel, Y. & Kanae, S. A global hydrological simulation to specify the sources of water used by humans. *Hydrol. Earth Syst. Sci.* **22**, 789–817 (2018).
16. Singh, R. & Kumar, R. Vulnerability of water availability in India due to climate change: a bottom-up probabilistic Budyko analysis. *Geophys. Res. Lett.* **42**, 9799–9807 (2015).
17. Rijdsberman, F. R. Water scarcity: fact or fiction? *Agric. Water Manag.* **80**, 5–22 (2006).
18. Liu, M. & Sun, A. A physical agricultural drought index based on root zone water availability: model development and application. *Geophys. Res. Lett.* **47**, <https://doi.org/10.1029/2020GL088553> (2020).
19. Ma, T. et al. Pollution exacerbates China's water scarcity and its regional inequality. *Nat. Commun.* **11**, 650 (2020).
20. Zhao, F. et al. Predicting the climate change impacts on water-carbon coupling cycles for a loess hilly-gully watershed. *J. Hydrol.* **581**, 124388 (2020).
21. Zhao, F. et al. The role of climate change and vegetation greening on evapotranspiration variation in the Yellow River Basin, China. *Agric. For. Meteorol.* **316**, 108842 (2022).
22. Jaeger, W. K. et al. Toward a formal definition of water scarcity in natural-human systems. *Water Resour. Res.* **49**, 4506–4517 (2013).
23. Huggins, X. et al. Hotspots for social and ecological impacts from freshwater stress and storage loss. *Nat. Commun.* **13**, 439 (2022).
24. Duan, R. et al. Stepwise clustering future meteorological drought projection and multi-level factorial analysis under climate change: a case study of the Pearl River Basin, China. *Environ. Res.* **196**, 110368 (2021).
25. Liu, S., Shi, H., Niu, J., Chen, J. & Kuang, X. Assessing future socioeconomic drought events under a changing climate over the Pearl River basin in South China. *J. Hydrol. Reg. Stud.* **30**, 100700 (2020).
26. Secci, D., Tanda, M. G., D'Oria, M., Todaro, V. & Fagandini, C. Impacts of climate change on groundwater droughts by means of standardized indices and regional climate models. *J. Hydrol.* **603**, 127154 (2021).
27. Omer, A., Zhuguo, M., Yuan, X., Zheng, Z. & Saleem, F. A hydrological perspective on drought risk-assessment in the Yellow River Basin under future anthropogenic activities. *J. Environ. Manag.* **289**, 112429 (2021).
28. Zhao, F. et al. Parameter uncertainty analysis of the SWAT model in a mountain-loess transitional watershed on the Chinese Loess Plateau. *WATER* **10**, 690 (2018).
29. Weaver, C. P. et al. Improving the contribution of climate model information to decision making: the value and demands of robust decision frameworks. *WIREs Clim. Change* **4**, 39–60 (2012).
30. Zhao, F. et al. Projected changes in population exposure to drought in China under CMIP6 forcing scenarios. *Atmos. Environ.* **282**, 119162 (2022).
31. Koppa, A., Alam, S., Miralles, D. G. & Gebremichael, M. Budyko-based long-term water and energy balance closure in global watersheds from earth observations. *Water Resour. Res.* **57**, e2020WR028658 (2021).
32. Konapala, G., Mishra, A. K., Wada, Y. & Mann, M. E. Climate change will affect global water availability through compounding changes in seasonal precipitation and evaporation. *Nat. Commun.* **11**, 3044 (2020).
33. Huang, Z., Yuan, X. & Liu, X. The key drivers for the changes in global water scarcity: water withdrawal versus water availability. *J. Hydrol.* **601**, <https://doi.org/10.1016/j.jhydrol.2021.126658> (2021).
34. Yin, Y. et al. Quantifying water scarcity in northern China within the context of climatic and societal changes and south-to-north water diversion. *Earth's Future* **8**, e2020EF001492 (2020).
35. Jiang, Y. China's water scarcity. *J. Environ. Manag.* **90**, 3185–3196 (2009).
36. He, F., Zhu, Y. & Jiang, S. In *Water Conservation and Wastewater Treatment in BRICS Nations* (eds Singh, P. et al.) 269–284 (Elsevier, 2020).
37. Vora, A. & Singh, R. Satellite based Budyko framework reveals the human imprint on long-term surface water partitioning across India. *J. Hydrol.* **602**, <https://doi.org/10.1016/j.jhydrol.2021.126770> (2021).
38. Cheng, S. et al. Improved understanding of how catchment properties control hydrological partitioning through machine learning. *Water Resour. Res.* **58**, e2021WR031412 (2022).
39. Shen, Q., Cong, Z. & Lei, H. Evaluating the impact of climate and underlying surface change on runoff within the Budyko framework: a study across 224 catchments in China. *J. Hydrol.* **554**, 251–262 (2017).
40. Chen, T., Zou, L., Xia, J., Liu, H. & Wang, F. Decomposing the impacts of climate change and human activities on runoff changes in the Yangtze River Basin: Insights from regional differences and spatial correlations of multiple factors. *J. Hydrol.* **615**, 128649 (2022).
41. Pokhrel, Y. et al. Global terrestrial water storage and drought severity under climate change. *Nat. Clim. Change* **11**, 226–233 (2021).
42. Marin-Ferrer, M., Vernaccini, L. & Poljansek, K. Index for risk management INFORM concept and methodology report—version 2017. *EUR 28655 EN* <https://doi.org/10.2760/094023> (2017).
43. Cardona, O.-D. et al. Determinants of risk: exposure and vulnerability. in *Managing the Risks of Extreme Events and Disasters to Advance Climate Change Adaptation. A Special Report of Working Groups I and II of the Intergovernmental Panel on Climate Change (IPCC)* (eds Field, C. B. et al.) 65–108 (Cambridge University Press, 2012).
44. Cutter, S. L. & Finch, C. Temporal and spatial changes in social vulnerability to natural hazards. *Proc. Natl Acad. Sci. USA* **105**, 2301–2306 (2008).
45. Zhang, Q. et al. Droughts across China: drought factors, prediction and impacts. *Sci. Total Environ.* **803**, 150018 (2022).
46. Song, L. et al. Divergent vegetation responses to extreme spring and summer droughts in Southwestern China. *Agric. For. Meteorol.* **279**, 107703 (2019).
47. Zhao, J., Zhang, Q., Zhu, X., Shen, Z. & Yu, H. Drought risk assessment in China: evaluation framework and influencing factors. *Geogr. Sustain.* **1**, 220–228 (2020).
48. Zhuo, L. et al. Volume versus value of crop-related water footprints and virtual water flows: a case study for the Yellow River Basin. *J. Hydrol.* **608**, 127674 (2022).
49. Zhou, F. et al. Deceleration of China's human water use and its key drivers. *Proc. Natl Acad. Sci. USA* **117**, 7702–7711 (2020).
50. Zhao, F., Ma, S. & Wu, Y. Changes in dry-season water availability and attributions in the Yellow River Basin, China. *Front. Environ. Sci.* **9**, 762137 (2021).
51. Fu, B. P. On the calculation of the evaporation from land surface. *Sci. Atmos. Sinica* **5**, 23 (1981).
52. Budyko, M. I. The heat balance of the Earth's surface. *Soviet Geography* **2**, 3–13 (1961).
53. Donohue, R. J., Roderick, M. L. & McVicar, T. R. On the importance of including vegetation dynamics in Budyko's hydrological model. *Hydrol. Earth Syst. Sci.* **11**, 983–995 (2007).
54. Zhang, L. et al. A rational function approach for estimating mean annual evapotranspiration. *Water Resour. Res.* **40**, <https://doi.org/10.1029/2003WR002710> (2004).
55. Xi, Y. et al. Trade-off between tree planting and wetland conservation in China. *Nat. Commun.* **13**, 1967 (2022).
56. Zhou, G. et al. Global pattern for the effect of climate and land cover on water yield. *Nat. Commun.* **6**, 5918, <https://doi.org/10.1038/ncomms6918> (2015).
57. Yin, G. et al. Multi-scale assessment of water security under climate change in North China in the past two decades. *Sci. Total Environ.* **805**, 150103 (2022).
58. Greve, P. et al. Global assessment of trends in wetting and drying over land. *Nat. Geosci.* **7**, 716–721 (2014).
59. Wei, X. et al. Vegetation cover—another dominant factor in determining global water resources in forested regions. *Global Change Biol.* **24**, 786–795 (2018).
60. Miao, C. et al. High-quality reconstruction of China's natural streamflow. *Sci. Bull.* **67**, 547–556 (2022).
61. Ghiggi, G., Humphrey, V., Seneviratne, S. I. & Gudmundsson, L. GRUN: an observation-based global gridded runoff dataset from 1902 to 2014. *Earth Syst. Sci. Data* **11**, 1655–1674 (2019).

62. Weaver, C. P. et al. Improving the contribution of climate model information to decision making: the value and demands of robust decision frameworks. *WIREs Clim. Change* **4**, 39–60 (2013).
63. Masson-Delmotte, V. et al. *IPCC, 2021: Climate Change 2021: The Physical Science Basis. Contribution of Working Group I to the Sixth Assessment Report of the Intergovernmental Panel on Climate Change* (Cambridge University Press, 2021).
64. Doblas-Reyes, F. J. et al. 2021: Linking global to regional climate change. in *Climate Change 2021: The Physical Science Basis. Contribution of Working Group I to the Sixth Assessment Report of the Intergovernmental Panel on Climate Change* (eds Masson-Delmotte, V. et al.). 1363–1512 (Cambridge University Press, Cambridge, 2021).
65. Konapala, G., Mishra, A. K., Wada, Y. & Mann, M. E. Climate change will affect global water availability through compounding changes in seasonal precipitation and evaporation. *Nat. Commun.* **11**, 3044 (2020).
66. Allan, R. P., Soden, B. J., John, V. O., Ingram, W. & Good, P. Current changes in tropical precipitation. *Environ. Res. Lett.* **5**, 025205 (2010).
67. Liu, C. & Allan, R. P. Observed and simulated precipitation responses in wet and dry regions 1850–2100. *Environ. Res. Lett.* **8**, 034002 (2013).
68. Donat, M. G., Lowry, A. L., Alexander, L. V., O’Gorman, P. A. & Maher, N. More extreme precipitation in the world’s dry and wet regions. *Nat. Clim. Change* **6**, 508–513 (2016).
69. Polson, D., Hegerl, G. C., Allan, R. P. & Sarojini, B. B. Have greenhouse gases intensified the contrast between wet and dry regions? *Geophys. Res. Lett.* **40**, 4783–4787 (2013).
70. He, C. et al. Future global urban water scarcity and potential solutions. *Nat. Commun.* **12**, 4667 (2021).
71. Breiman, L. Random forests. *Machine Learning* **45**, 5–32 (2001).
72. Grömping, U. Variable importance assessment in regression: linear regression versus random forest. *Am. Stat.* **63**, 308–319 (2009).
73. Schoppa, L., Disse, M. & Bachmair, S. Evaluating the performance of random forest for large-scale flood discharge simulation. *J. Hydrol.* **590**, 125531 (2020).
74. Li, Z. & Quiring, S. M. Projection of streamflow change using a time-varying Budyko framework in the contiguous United States. *Water Resour. Res.* **58**, e2022WR033016 (2022).
75. Gaines, M. D., Tulbure, M. G. & Perin, V. Effects of climate and anthropogenic drivers on surface water area in the southeastern United States. *Water Resour. Res.* **58**, e2021WR031484 (2022).
76. Chinnasamy, C. V. et al. Characterization of municipal water uses in the contiguous United States. *Water Resour. Res.* **57**, e2020WR028627 (2021).
77. Padrón, R. S., Gudmundsson, L., Greve, P. & Seneviratne, S. I. Large-scale controls of the surface water balance over land: insights from a systematic review and meta-analysis. *Water Resour. Res.* **53**, 9659–9678 (2017).
78. Jiang, C. et al. Separating the impacts of climate change and human activities on runoff using the Budyko-type equations with time-varying parameters. *J. Hydrol.* **522**, 326–338 (2015).
79. Xing, W., Wang, W., Shao, Q. & Yong, B. Identification of dominant interactions between climatic seasonality, catchment characteristics and agricultural activities on Budyko-type equation parameter estimation. *J. Hydrol.* **556**, 585–599 (2018).
80. Li, D., Pan, M., Cong, Z., Zhang, L. & Wood, E. Vegetation control on water and energy balance within the Budyko framework. *Water Resour. Res.* **49**, 969–976 (2013).
81. Saha, A., Joseph, J. & Ghosh, S. Climate controls on the terrestrial water balance: influence of aridity on the basin characteristics parameter in the Budyko framework. *Sci. Total Environ.* **739**, 139863 (2020).
82. Sinha, J., Jha, S. & Goyal, M. K. Influences of watershed characteristics on long-term annual and intra-annual water balances over India. *Journal of Hydrology* **577**, 123970 (2019).
83. Wang, D. & Hejazi, M. Quantifying the relative contribution of the climate and direct human impacts on mean annual streamflow in the contiguous United States. *Water Resour. Res.* **47**, 10 (2011).
84. Bai, P., Liu, X., Zhang, D. & Liu, C. Estimation of the Budyko model parameter for small basins in China. *Hydrol. Processes* **34**, 125–138 (2020).
85. Lei, Y., Wang, J. A., Yue, Y., Zhou, H. & Yin, W. Rethinking the relationships of vulnerability, resilience, and adaptation from a disaster risk perspective. *Nat. Hazards* **70**, 609–627 (2014).
86. Turner, B. L. et al. A framework for vulnerability analysis in sustainability science. *Proc. Natl Acad. Sci. USA* **100**, 8074–8079 (2003).
87. Cardona, O. D. & Carreño, M. L. Updating the indicators of disaster risk and risk management for the Americas. *J. Integr. Disaster Risk Manag.* **1**, 27–47 (2011).
88. UNISDR. Terminology on Disaster Risk Reduction. http://www.unisdr.org/files/7817_UNISDRTerminologyEnglish.pdf. (2009) Accessed 6 June 2016.
89. Varis, O., Taka, M. & Kummu, M. The planet’s stressed river basins: too much pressure or too little adaptive capacity. *Earths Future* **7**, 1118–1135 (2019).
90. Kummu, M., Taka, M. & Guillaume, J. H. A. Gridded global datasets for Gross Domestic Product and Human Development Index over 1990–2015. *Sci. Data* **5**, 180004 (2018).
91. He, J. et al. The first high-resolution meteorological forcing dataset for land process studies over China. *Sci. Data* **7**, 25 (2020).
92. Penman, H. L. Natural evaporation from open water, bare soil and grass. *Proc. Royal Soc. Lond. Ser. A. Math. Phys. Sci.* **193**, 120 (1948).
93. Monteith, J. Evaporation and environment. *Symp. Soc. Exp. Biol.* **19**, 205–234 (1965).
94. Allen, R. G., Pereira, L. S., Raes, D. & Smith, M. Crop evapotranspiration. Guidelines for computing crop water requirements. pp. D05109 (Food and Agricultural Organisation of the United Nations, Rome, 1998).
95. Zhang, K. et al. Satellite based analysis of northern ET trends and associated changes in the regional water balance from 1983 to 2005. *J. Hydrol.* **379**, 92–110 (2009).
96. Pang, X. et al. Long term variation of evapotranspiration and water balance based on upscaling eddy covariance observations over the temperate semi-arid grassland of China. *Agric. For. Meteorol.* **308–309**, 108566 (2021).
97. Singh, R. & Kumar, R. The suitability of water scarcity indicators to the Indian context. *Water Security* **14**, 100097 (2021).
98. Xu, X., Liu, W., Scanlon, B. R., Zhang, L. & Pan, M. Local and global factors controlling water-energy balances within the Budyko framework. *Geophys. Res. Lett.* **40**, 6123–6129 (2013).

Acknowledgements

This study was funded by the National Natural Science Foundation of China (42101029 and 42271025), the China Postdoctoral Science Foundation (2022T150513 and 2020M683451), the National Key Research and Development Program of China (2022YFF1302200), the Innovation Team of Shaanxi Province (2021TD-52), Shaanxi Key Research and Development Program (2022ZDLSF06-04), and the Strategic Priority Research Program of Chinese Academy of Sciences (XDB40020205). F.B.Z. also thanks Neale Alan Hudson from the National Institute of Water & Atmospheric Research Limited, New Zealand, for polishing English during the preparation of this manuscript.

Author contributions

F.Z. conceived the idea and designed the research. X.W. carried out data analysis. F.Z. and Y.W. prepared the original draft and all authors reviewed the manuscript. S.K.S. provided constructive comments on the initial manuscript.

Competing interests

The authors declare no competing interests.

Additional information

Supplementary information The online version contains supplementary material available at <https://doi.org/10.1038/s43247-023-00808-3>.

Correspondence and requests for materials should be addressed to Yiping Wu.

Peer review information *Communications Earth & Environment* thanks Jia Qin and the other, anonymous, reviewer(s) for their contribution to the peer review of this work. Primary Handling Editor: Aliénor Lavergne.

Reprints and permission information is available at <http://www.nature.com/reprints>

Publisher’s note Springer Nature remains neutral with regard to jurisdictional claims in published maps and institutional affiliations.



Open Access This article is licensed under a Creative Commons Attribution 4.0 International License, which permits use, sharing, adaptation, distribution and reproduction in any medium or format, as long as you give appropriate credit to the original author(s) and the source, provide a link to the Creative Commons license, and indicate if changes were made. The images or other third party material in this article are included in the article’s Creative Commons license, unless indicated otherwise in a credit line to the material. If material is not included in the article’s Creative Commons license and your intended use is not permitted by statutory regulation or exceeds the permitted use, you will need to obtain permission directly from the copyright holder. To view a copy of this license, visit <http://creativecommons.org/licenses/by/4.0/>.

© The Author(s) 2023